

COMBUSTION OF DAMAGED HIGH EXPLOSIVES

S. F. Son, H. L. Berghout, C. B. Skidmore, D. J. Idar, and B. W. Asay
Los Alamos National Laboratory
Los Alamos, NM 87545, U.S.A.

ABSTRACT

Impact or thermal ignition of high explosives, HE, results in deformation that can lead to damage. Fracture or defects, combined with sufficiently high pressure, dramatically increases the available surface area and potentially changes even the mode of combustion. Recent impact and cookoff experiments on PBX 9501, (HMX, octahydro-1,3,5,7-tetranitro-1,3,5,7-tetrazocine, with a binder), have shown complex cracking patterns caused by impact or pressurization. Fast reactive waves have been observed to propagate through the cracks at hundreds of meters per second. We present experiments that examine the combustion of mechanically and thermally damaged samples of PBX 9501. Mechanically damaged samples, damaged by quasi-static pressing, exhibit large, $\sim 200 \mu\text{m}$ stress fracture accompanied by extensive rubblization. Combustion experiments determine a $1.4 \pm 0.6 \text{ MPa}$ critical pressure for the onset of violent convective combustion, consistent with connected porosity of $25 \mu\text{m}$. Thermally damaged samples, damaged by heating in a 180°C oven for 30 minutes, exhibit $2\text{-}20 \mu\text{m}$ widely distributed cracking. Combustion experiments indicate a $9.2 \pm 0.4 \text{ MPa}$ critical pressure for the onset of violent convective combustion, consistent with connected porosity of $4 \mu\text{m}$. The burn rate and pressure exponent of thermally damaged PBX 9501 are similar to those of the pristine material.

INTRODUCTION

The shift from conductive or normal burning to convective burning is an important step of the deflagration-to-detonation transition in explosives and other energetic materials.¹⁻³ Normal deflagration involves primarily conductive heat transfer from the gas-phase flame region to the surface, and to a lesser extent, radiation transport from the gas to the solid. In contrast, convective burning involves heat transfer augmented by mass flow. Defects increase the available surface area where combustion can occur and is necessary for convective burning in energetic materials. The effect of defects on combustion has major implications for the safety and reliability of energetic materials.

Voids and cracks in explosives may result from numerous environmental and physical factors. Impact, aging, and variations in temperature and pressure associated with combustion are a few of the factors that can produce defects. At sufficiently high pressures, the surface area of a defect becomes accessible to deflagration. Defects can trap the hot reaction products, creating the necessary pressure gradient for convective burning. There exist numerous studies on the effects of voids and cracks on the combustion of some common propellants^{3,4}, but relatively few studies exist of the effects of voids and cracks on the combustion of high explosives.³ Ramaswamy and Field have studied hot spot and crack propagation in single crystals of RDX.⁵ Explosives such as HMX, (octahydro-1,3,5,7-tetranitro-1,3,5,7-tetrazocine), typically use a binder that makes it possible to shape the explosive. Binder affects the number, shape, and size of voids, as well as influences somewhat the combustion.⁶

Recent experiments highlight the importance of cracks and voids in the ignition, combustion, and

DISCLAIMER

This report was prepared as an account of work sponsored by an agency of the United States Government. Neither the United States Government nor any agency thereof, nor any of their employees, make any warranty, express or implied, or assumes any legal liability or responsibility for the accuracy, completeness, or usefulness of any information, apparatus, product, or process disclosed, or represents that its use would not infringe privately owned rights. Reference herein to any specific commercial product, process, or service by trade name, trademark, manufacturer, or otherwise does not necessarily constitute or imply its endorsement, recommendation, or favoring by the United States Government or any agency thereof. The views and opinions of authors expressed herein do not necessarily state or reflect those of the United States Government or any agency thereof.

DISCLAIMER

Portions of this document may be illegible in electronic image products. Images are produced from the best available original document.

by Idar *et al.*⁷ The Steven Test determines the critical impact velocity of an energetic material to the low-speed impact of a blunt steel projectile. Radial cracks emanating from the impact point are apparent in Fig. 1 for a test where no sustained reaction occurred. Idar *et al.* find that damaged PBX 9501 has a significantly lower impact threshold for violent reaction than pristine material.

Henson *et al.* have conducted shear impact experiments using thin disks of PBX 9501.⁸ They drive a rectangular steel plunger into the lightly confined disk at about 100 m/s. Plunger intrusion causes both shear and non-shear fracturing with reaction initiated along fracture zones as shown in Fig. 2. Skidmore *et al.* have used visible microscopy to study damaged samples recovered from the shear impact experiments and find that the HMX along the fracture zones shows clear signs of heating and quenched reaction.⁹

Evidence of the importance of combustion in cracks also appears in elevated-temperature experiments, such as Mechanically Coupled Cookoff, MCCO. Dickson *et al.* slowly heat a confined sample of PBX 9501 to a well-defined temperature then ignite the sample. They detect reaction, indicated by luminous emission, throughout intricate networks of cracks that are caused by pressurization due to production of reactive gases.¹⁰ Figure 3 shows luminous reaction in cracks during an MCCO experiment. The fast reactive waves, indicated by the luminosity, propagate through the cracks at velocities on the order of 500 m/s.

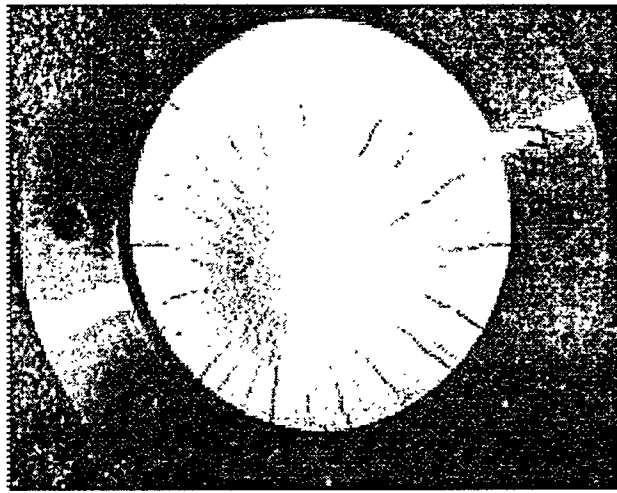
Precisely machined slots in PBX 9501 allowed us to examine the propagation of fast reactive waves in cracks of PBX 9501, focusing on the reactive wave velocity and on the interplay of pressure and crack size the role of pressure and defect size on convective burning in PBX 9501.¹¹ Experiments at initial pressures of 6.0 MPa reveal monotonic reactive wave propagation velocities around 7 m/s for a 100- μ m slot. We observe reactive wave velocities as high as 100 m/s in experiments at initial pressures of 17.2 MPa and various slot widths. Similar experiments at lower pressure exhibit oscillatory reactive wave propagation in the slot with periodic oscillations whose frequencies vary with combustion vessel pressure. Threshold pressure experiments for combustion propagation into closed-end slots of PBX 9501 find that combustion propagates into 2-mm, 1-mm, 100- μ m, 50- μ m, and 25- μ m slots at approximately 0.1, 0.2, 0.9, 1.6, and 1.8 MPa, respectively.

Maienschein and Chandler report erratic burn rates in HMX-based explosives with low binder content (~5 wt%), but observe no such erratic rapid burn rates for similar explosives with greater binder content (15 wt%) over the range of pressures considered.¹² Similar experiments by Son *et al.* visually observed erratic burn rates in high-nitrogen compounds. Video records verify that erratic burn rates result from reaction propagating into very small cracks that were present in the sample.¹³ This observation is consistent with the Maienschein and Chandler experiment where smaller amounts of binder make defects and voids more likely, leading to the reported erratic burn rates. Our current efforts examine the effects of thermally and mechanically induced damage on reaction violence in PBX 9501. Our studies investigate the effects of voids and cracks on the combustion of PBX 9501 (HMX with an estane-based binder). In addition to improving our understanding of the safety aspects related to PBX 9501, these experiments provide useful data for current efforts to develop understanding and improved models of violent, explosive reactions.

EXPERIMENTAL SETUP

Mechanically damaged samples were obtained from PBX 9501 molding powder that was hydrostatically pressed to about 1.825 g/cm³ then machined into 0.9525-cm diameter by 1.905-cm long cylindrical pellets. An Instron 5567 Mechanical Testing Workstation with a 30-kN load cell quasi-statically compressed the pellets at constant crosshead speeds of 1.27-12.7 cm/min to the point of specimen failure resulting in macrocracking along the shear cones through the specimens and diamond shear cracking patterns on the outer surfaces.

We prepare thermally damaged PBX 9501 samples by axially pressing molding powder into cylindrical pellets approximately one-centimeter tall and one-centimeter in diameter with an average density of 1.81 g/cm³. Pellets are then heated unconfined in a 180° C oven for 30 minutes then allowed to cool to room temperature. Nd³⁺:YAG-laser-based Second-Harmonic-Generation (SHG) and microscopy confirms that heating entirely converts normal β -phase HMX crystals to δ -phase crystals.¹⁴



RECEIVED
DEC 13 2000
OSTI

Figure 1. PBX 9501 target showing the extensive radial cracking around the impact point that results from low speed impact by a hemispherical blunt projectile, from Idar *et al.*⁷ The cover plate has been removed to view the explosive

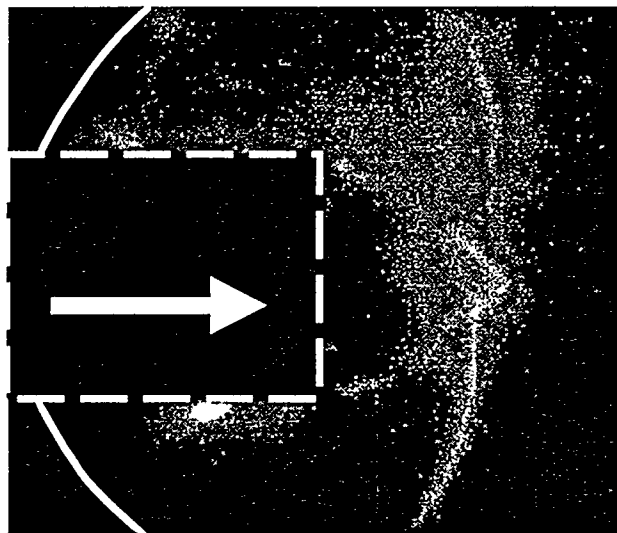


Figure 2. Ignition of PBX 9501 initiated by shearing-projectile impact from Henson *et al.*⁸ The solid curved line approximately outlines the disk of PBX 9501 while the dashed box outlines the projectile that has impacted the disk from the left. Luminous reaction is seen along the edge of the projectile, in the shear wedge (approximately 2D experiment) in front of the projectile, and in other stress cracks caused by the impact.

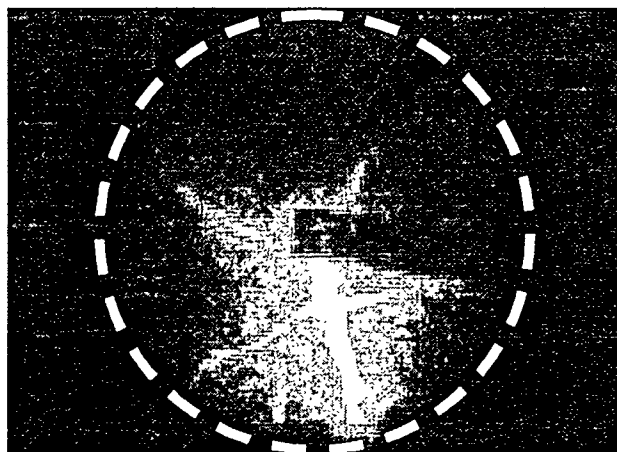


Figure 3. Luminous reaction in cracks of PBX 9501 during mechanically coupled cookoff experiment from Dickson *et al.*¹⁰ The dashed line approximately outlines the disk of PBX 9501. The dark rectangular area intruding from the right is a foil sheet used for sample ignition. Ignition of a hole at the center of the sample with a hot NiCr wire pressurizes the sample causing cracking, and luminous reaction can be seen in these cracks.

Microscopic analysis provides an estimate of the extent and characterizes the damage present in the pellets. Mechanically and thermally damaged samples were cut along the cylinder axis and vacuum-mounted in low-viscosity epoxy for viewing in cross-section. The specimens were further prepared for examination in reflected, plane-polarized light by polishing with a sequence of fine abrasives. A previous report describes the procedural details.¹⁵ No etching or staining was necessary. Plane-polarized-light microscopy using a Leica DMRXA microscope with a Diagnostic Instruments spot camera produced digital images of the damage. The spatial resolution of the microscope optics was matched with the camera pixel characteristics to nearly meet the Nyquist limit in each case.

The combustion experiments are done in a two-liter stainless-steel-pressurized combustion vessel. The combustion vessel provides four optical access ports, allowing visual observation of experiments at pressures up to 21 MPa. All experiments are conducted with the pressure vessel and sample initially at room temperature, ~293 K. Clear epoxy prevents combustion from spreading down the sides of the pellets.

We use several diagnostic tools to monitor combustion. A Canon XL-1 digital video system records the entire experiment at 30 fps and a Red Lake MotionScope PCI 8000S high-speed-video system provides up to eight seconds of images at frame rates up to 8,000 fps. An Omega Model PX605-10KGI pressure transducer monitors the pressure in the combustion vessel, while the PCB Piezotronics Model 113A23 pressure sensors monitor the transient combustion-vessel pressure and the pressure of the slot relative to the combustion vessel. Tektronix Model TDS 460A and TDS 540A digital oscilloscopes capture the pressure sensor outputs for later storage and analysis.

RESULTS AND DISCUSSION

Mechanically Damaged High Explosives

Microscopic studies of mechanically damaged samples reveal extensive cracking and regions of 'rubblization'. Figure 4 shows images of a mechanically damaged sample sliced along the pellet's cylindrical axis. The low magnification view, top, shows shear cones, characteristic of compression testing, with large cracks along the margins that form a large 'X'. Higher magnification views, bottom, show details of the upper right hand leg of the 'X' and the central region of extensive damage where the shear cones approach. Average large crack width is about 200 μm though some areas are wider while other areas appear to be nearly blocked as shown in the Fig. 4. Near the center of the pellet where the shear cones merge, fine debris replaces the large cracks. The connected porosity in this region is sufficient to allow the mounting epoxy to flow into it, resulting in the darkening that is apparent around the shear cones. The epoxy does not enter and darken the regions away from the margins of the shear cones where little damage has occurred.

Combustion experiments were designed to observe the reaction of mechanically damaged pellets at a series of pressures to determine the threshold pressure necessary to produce violent reaction. Figure 5 presents a sequence of images showing the combustion of a mechanically damaged sample and Fig. 6 plots combustion vessel pressure versus time for the image sequence. The sample is ignited on the left in these images and deflagration progresses to the right. The first frame shows the sample prior to the experiment. The second frame shows normal burning following sample ignition, with the damage appearing to affect the curvature. The third frame shows luminous reaction in a crack ahead of the normally burning surface, the fourth frame shows brighter reaction in more cracks, and the fifth frame shows the entire pellet being consumed in the reaction. Combustion vessel pressure climbs gradually during the period of normal burning then rises rapidly when convective combustion enters and begins to consume the voids in the pellet.

We observe a critical pressure for violent reaction of our mechanically damaged samples of 1.4 ± 0.6 MPa. Below this pressure, damaged pellets burn in a normal, planar manner, while above this pressure, reaction enters the cracks and voids in the pellet, resulting in violent, convective burning. The plot in Fig. 7 displays the results of our previously reported critical pressure measurements for reaction entering machined-closed-end slots in PBX 9501.¹³ A simplified theoretical expression proposed by Belyaev *et al.* describes the interdependence of the critical pressure and the slot width³

$$p_c^{1+2n} w^2 = \text{constant}, \quad (1)$$

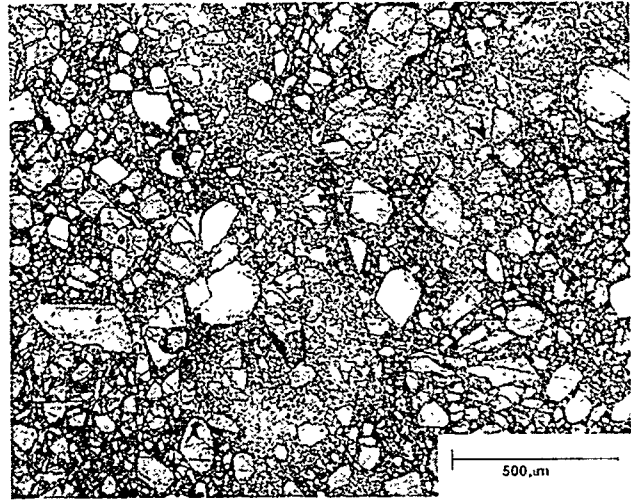
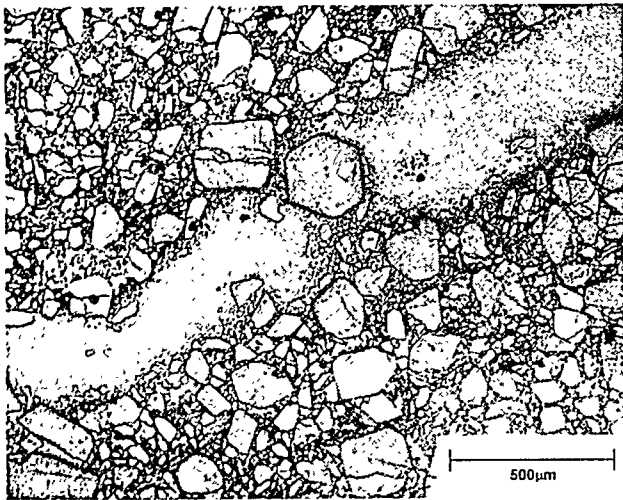


Figure 4. Images of a mechanically damaged sample sliced along the cylindrical axis. Top is a low magnification view of the mounted sample. Lower left is a higher magnification view of the upper-right-hand portion of the sample. Lower right is a higher magnification view of the central portion of the sample.

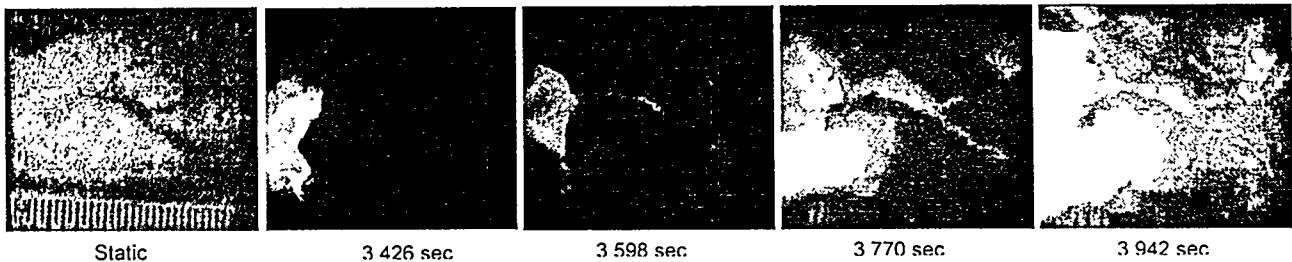


Figure 5. Sequence of images showing the combustion of a mechanically damaged sample.

where p_c is the critical pressure, n is the conductive burn rate pressure exponent and w is the slot width. The dashed line in Figure 7 results from Equation 1 where we have assumed n to equal 0.92, the value for PBX 9501,¹³ and the constant equal to 8×10^8 in SI units. The critical pressure for violent reaction in our current results suggest that the mechanically damaged samples have an effective defect and crack width of about 25 μm . Effective defect dimensions determined from our critical-pressure experiments are much smaller than the $\sim 200\text{-}\mu\text{m}$ cracks along the shear cone margins observed by microscopy. This is probably because the narrowest passage in the cracks must be accessed by the flame before convective burning can be fully established. In other words, the fine scale connected porosity of the damage appear to control the spread of the flame into the crack. Furthermore, the surface area of the large cracks is much less than the surface area of the fine scale damage that is only accessible at higher pressures. Truly violent reaction occurs when the pressure allows burning to occur in the debris region around the large cracks and in the center of the pellet. The large cracks provide access for combustion to reach the porous debris regions but do not contribute much to reaction violence.

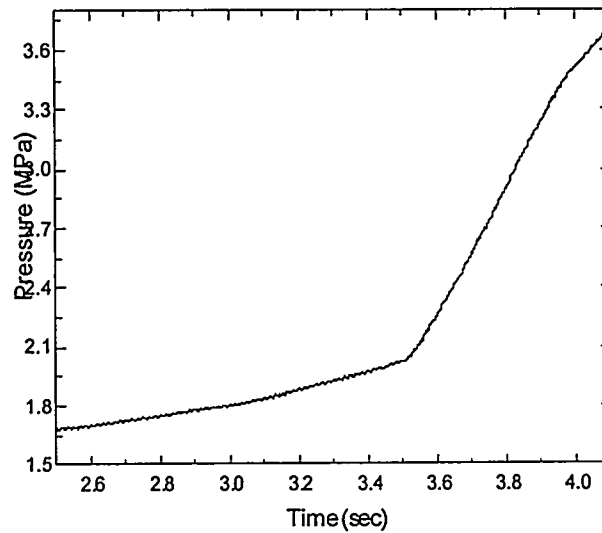


Figure 6. Plot of pressure vs. time for combustion of a mechanically damaged sample.

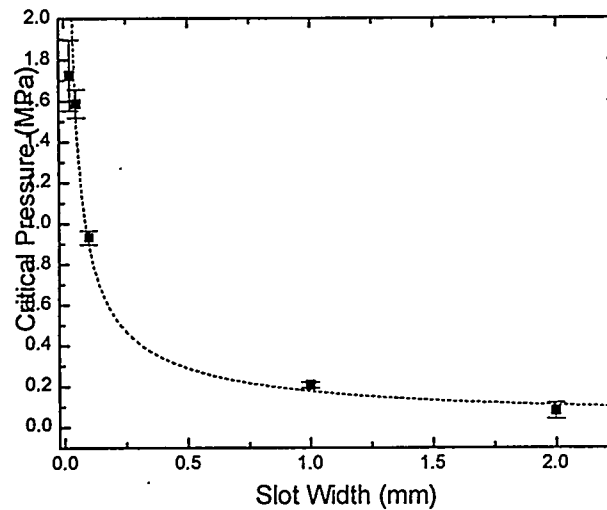


Figure 7. Plot of critical pressure vs. slot width for PBX 9501.

Thermally Damaged High Explosives

Microscopic studies of thermally damaged samples reveal extensive cracking, uniformly distributed throughout the pellet. Figure 8 shows images of a thermally damaged sample sliced along the pellet's cylindrical axis. The low magnification view, top, shows the uniformly distributed nature of the thermal damage. The higher magnification views, bottom, compare a pellet that has not been heated, left, with one that has been heated in a 180° C oven for 30 minutes, right. Individual HMX crystals and binder regions, which are clearly identifiable in the unheated sample, are difficult to identify in the heated samples. Large, 2 - 20 μm cracks are randomly distributed throughout the heat-treated sample, but are not identifiable in the unheated sample. Nd³⁺:YAG-laser-based Second-Harmonic-Generation (SHG) and microscopy confirms that heating entirely converts the normal β -phase HMX crystals to δ -phase crystals.¹⁴ Expansion due to heating and the β - δ phase transition changes the crystalline structure and produces fractures and voids throughout

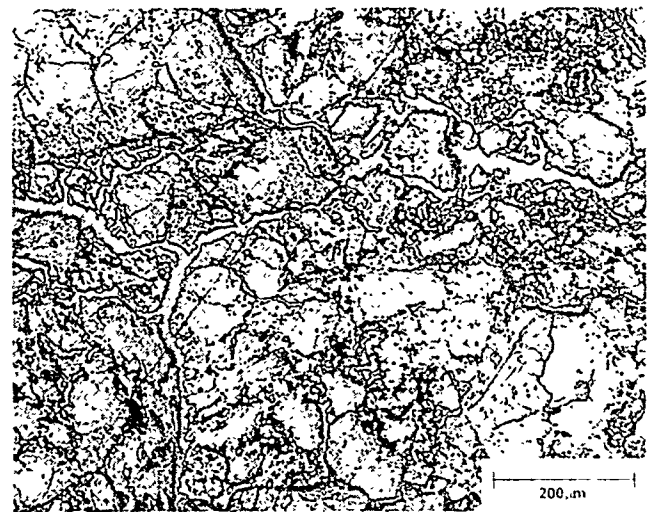
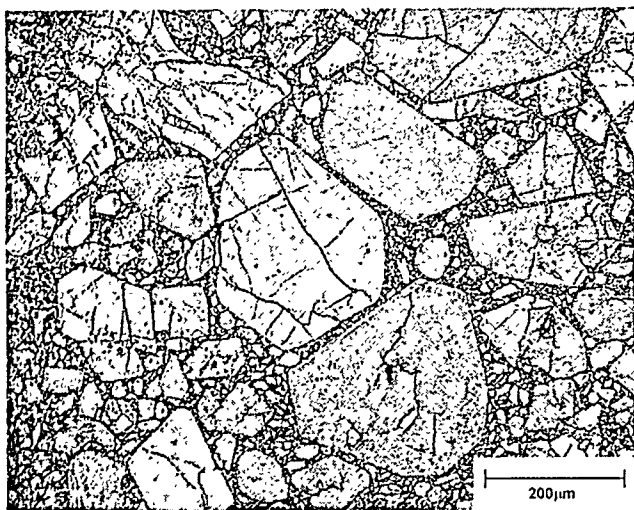
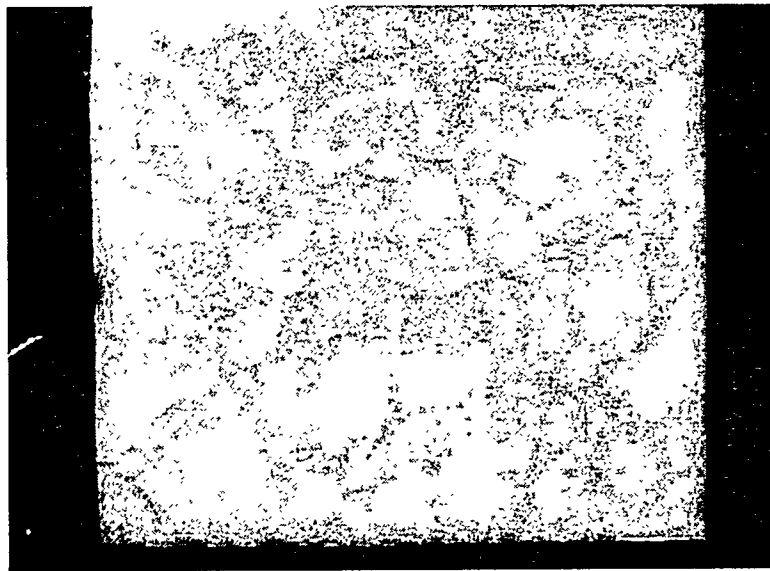


Figure 8. Images for the thermal-damaged sample sliced along the cylindrical axis. Top is a low magnification view of the mounted sample. Lower left is higher-magnification view of a pristine PBX 9501 sample. Lower right is a higher-magnification view of a sample that has been heated in a 180° oven for thirty minutes.

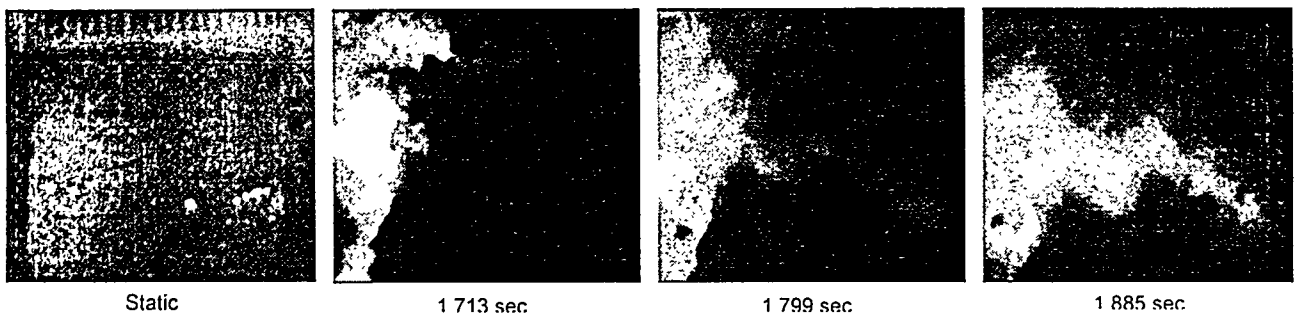


Figure 9. Sequence of images showing the combustion of a mechanically damaged sample.

the pellets. Large cracks appear to follow the boundaries that existed between crystals prior to heating. The very small crystals, present in the binder between the large crystals in the unheated sample, are not present after heating, and the large areas of HMX no longer have sharp crystalline faces. This may be caused by solvation of HMX crystals in the binder during heating, followed by some recrystallization during cooling.

Combustion experiments of thermally damaged pellets at a series of pressures were performed to determine the threshold pressure necessary to produce violent reaction. Figure 9 is a sequence of images showing the combustion of a thermally damaged sample and Fig. 10 plots combustion vessel pressure versus

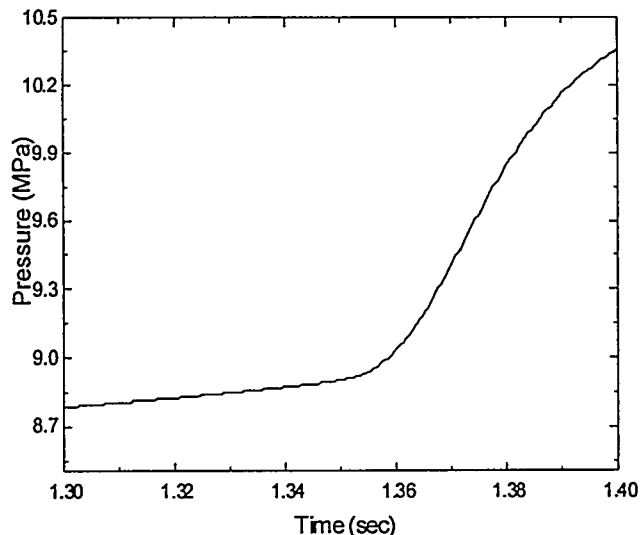


Figure 10. Plot of pressure vs. time for combustion of a mechanically damaged sample.

time for the image sequence. The sample is ignited on the left in these images and deflagration progresses to the right. The first frame shows the sample prior to the experiment. The second frame shows normal burning following sample ignition. The third frame shows luminous reaction in a crack ahead of the normally burning surface and the fourth frame shows brighter reaction in the crack as reaction progresses and the surface of the crack regresses. Combustion vessel pressure climbs gradually during the period of normal burning then rises rapidly when convective combustion enters and begins to consume the voids in the pellet.

We observe a critical pressure for violent reaction of our thermally damaged samples of 9.2 ± 0.4 MPa. Below this pressure, damaged pellets burn in a normal, planar manner, while above this pressure, reaction enters the cracks and voids in the pellet, resulting in violent, convective burning. Convective burning was observed in 10 thermally damaged samples. A planar front was *never* observed during these violent burns. This has significant modeling implications. Following the analysis above for the mechanically damaged samples, the critical pressure for violent reaction in our current results suggest that the thermally damaged samples have an effective defect and crack width of about $4 \mu\text{m}$. This is in the low end of the range of the microscopically observed damage noted above. Again, the smaller widths of the crack appear to control the onset to convective burning. Additionally, below the threshold for violent reaction, we find that the normal burn rate and pressure exponent of the heat-damaged samples are similar (within about 10%) to those for undamaged samples. We plan to follow this study with a real time microscopic examination of PBX 9501 heating to illuminate the significant changes that we observe between heated and pristine materials.

CONCLUSION

Mechanically damaged samples, damaged by quasi-static pressing, exhibit large, 200-300 μm stress fracture accompanied by extensive rubblization. Combustion experiments determine a 1.4 ± 0.6 MPa critical pressure for the onset of violent convective combustion, consistent with 25- μm connected porosity. Thermally damaged samples, damaged by heating in a 180° C oven for 30 minutes, exhibit 2-20 μm randomly distributed cracking. Combustion experiments find a 9.2 ± 0.4 MPa critical pressure for the onset of violent convective combustion, consistent with connected porosity of 4 μm . The smaller length-scales of the connected porosity appear to control the onset of convective burning. In even the thermal damaged material, which has quite uniformly distributed damage, convective burning is observed to propagate in a very nonplanar fashion. These results have implications to modeling efforts. The burn rate and pressure exponent of thermally damaged PBX 9501 are similar to those of the pristine material below the critical pressure. Future work should include combustion driven cracks and the combustion of partially decomposed materials.

ACKNOWLEDGEMENTS

We acknowledge the support of Los Alamos National Laboratory, under contract W-7405-ENG-36. In particular, we acknowledge the support of the Laboratory Directed Research and Development Program of Los Alamos National Laboratory.

1. B. W. Asay, S. F. Son, and J. B. Bdzil, *International Journal of Multiphase Flow* 22:923-952 (1996).
2. A. F. Belyaev and V. K. Bobolev, *Transition From Deflagration to Detonation in Condensed Phases*, 1975 translation ed. (National Technical Information Service, Springfield, VA, 1973).
3. H. H. Bradley and T. L. Boggs, "Convective Burning in Propellant Defects: A Literature Review," Naval Weapons Center, China Lake, CA Report No. NWC-TP-6007, 1978.
4. M. Kumar and K.K. Kuo, in *Fundamentals of Solid Propellant Combustion*, (K. Kuo and M. Summerfield, Eds.) AIAA, Inc., New York, 1984, Vol. 90, pp. 339-350.
5. A. L. Ramaswamy and J. E. Field, *Journal of Applied Physics* 79:3842-3847 (1996).
6. S. F. Son, H. L. Berghout, C. A. Bolme *et al.*, *The Twenty-Eighth International Symposium on Combustion*, The Combustion Institute, Edinburgh, Scotland, 2000.
7. D. J. Idar, J. W. Straight, M. A. Osborn *et al.*, *Shock Compression of Condensed Matter -- 1999*, American Institute of Physics, Snowbird, Utah, 1999.
8. B. F. Henson, B. W. Asay, P. M. Dickson *et al.*, *11th International Detonation Symposium*, Snowmass, Colorado, 1998.
9. C. B. Skidmore, D. S. Phillips, B. W. Asay *et al.*, *Shock Compression of Condensed Matter -- 1999*, American Institute of Physics, Snowbird, Utah, 1999.
10. P. M. Dickson, B. W. Asay, B. F. Henson *et al.*, *11th International Detonation Symposium*, Snowmass, Colorado, 1998.
11. H. L. Berghout, S. F. Son, and B. W. Asay, *1999 JANNAF PSHS Meeting*, Cocoa Beach, Florida, 1999.
12. J. L. Maienschein and J. B. Chandler, *11th International Detonation Symposium*, Snow Mass, Colorado, 1998.
13. S. F. Son, H. L. Berghout, C. A. Bolme *et al.*, *1999 JANNAF PSHS Meeting*, Cocoa Beach, Florida, 1999.
14. B. F. Henson, B. W. Asay, R. K. Sander *et al.*, *Physical Review Letters* 82:1213-1216 (1999).
15. C. B. Skidmore, D. S. Phillips, and N. B. Crane, *Microscope* 45:127-136 (1997).

GENERAL DISCLAIMER

This document may have problems that one or more of the following disclaimer statements refer to:

- ❖ This document has been reproduced from the best copy furnished by the sponsoring agency. It is being released in the interest of making available as much information as possible.
- ❖ This document may contain data which exceeds the sheet parameters. It was furnished in this condition by the sponsoring agency and is the best copy available.
- ❖ This document may contain tone-on-tone or color graphs, charts and/or pictures which have been reproduced in black and white.
- ❖ This document is paginated as submitted by the original source.
- ❖ Portions of this document are not fully legible due to the historical nature of some of the material. However, it is the best reproduction available from the original submission.